

Interaction Forces between BSA Layers Adsorbed on Silica Surfaces Measured with an Atomic Force Microscope

Juan J. Valle-Delgado,[†] José A. Molina-Bolívar,[‡] Francisco Galisteo-González,^{*,†} María J. Gálvez-Ruiz,[†] Adam Feiler,[§] and Mark W. Rutland[§]

Biocolloid and Fluid Physics Group, Department of Applied Physics, Science Faculty, University of Granada, 18071 Granada, Spain, Department of Applied Physics II, University Polytechnic School, University of Málaga, 29013 Málaga, Spain, and Department of Chemistry, Surface Chemistry, Royal Institute of Technology, and Institute for Surface Chemistry, 100 44 Stockholm, Sweden

Received: November 10, 2003; In Final Form: February 11, 2004

The interaction forces between bovine serum albumin (BSA) layers adsorbed on silica surfaces have been measured using an atomic force microscope (AFM) in conjunction with the colloid probe technique. Measurements of force–distance curves were made at different pH values and electrolyte concentrations (NaCl and CaCl₂). The interaction at long range is dominated by electrical double-layer forces, while at short surface separations an additional repulsion due to the compression of the adsorbed protein layers appears. However, prior to this steric interaction, when the pH is above the isoelectric point of the protein and at high salt concentration, a non-DLVO repulsive interaction is observed. This behavior is explained if the presence of hydration forces in the system is assumed. Theoretical predictions including a hydration term in the DLVO theory fit the experimental results satisfactorily. The results presented in this article provide a direct confirmation that the AFM colloid probe technique can provide a useful way of directly quantifying the interaction of biological macromolecules.

I. Introduction

Proteins occupy a dominant position within biotechnology because they are the most abundant organic molecules found in living systems.¹ Protein adsorption onto solid surfaces is important in many industrial and medical processes. In medical prostheses it is important to prevent blood protein adsorption and hence to reduce the risk of unwanted blood clotting.² Indeed one method of preventing blood clotting on medical implants is to actively encourage albumin adsorption; this concomitantly prohibits the adsorption of more harmful proteins such as IgG or fibrinogen.³ In cosmetics, pharmaceuticals, and food products proteins are often used as emulsifiers and/or stabilizers in colloidal dispersion. A fundamental understanding of protein–protein and protein–surface interactions is important to optimize the processes of production, purification, storage, and application of proteins.⁴

For the last two decades the surface force apparatus (SFA)⁵ has provided the opportunity to measure interaction forces between macroscopic surfaces in a liquid environment. This technique has demonstrated the validity of the DLVO (Derjaguin–Landau–Verwey–Overbeek) theory,^{6,7} which states that the total interaction force between two lyophobic particles in a medium can be expressed as a sum of the electrical double-layer force and the van der Waals force. The SFA results suggest that the theory describes satisfactorily the interaction forces between many surfaces immersed in electrolyte solution. However, some studies conducted in aqueous media showed the existence of forces not considered in the DLVO theory.^{8–16}

Derjaguin and Churaev¹⁷ proposed, therefore, that DLVO theory is applicable only to those surfaces whose water contact angle are in the range of 15°–64°. When the angle is outside this range, the DLVO theory may be extended to include the contribution from the extraneous forces. These forces are referred as hydration forces when the surfaces are hydrophilic, and they are correlated with the structure of water molecules and hydrated cations adsorbed on the surface. These forces can be strong enough to prevent the direct contact of surfaces at the primary minimum predicted by the classical DLVO theory. Despite the importance of these phenomena, the exact nature and mechanism of the hydration forces are still poorly understood.

The atomic force microscope (AFM) has become popular for measuring the interaction forces between two surfaces in a direct way. The applicability of the technique is evidenced by the wide variety of surfaces that have been investigated since the first studies in 1991.^{12,18} In SFA measurements, transparent, smooth and large surfaces are required, but there is not such limitation in AFM measurements. In the colloid probe technique the AFM is used to measure the interaction between a flat surface and a small spherical particle glued to the end of a cantilever. The interaction forces measured in this way can be appropriately compared with theory and with the results obtained from other force measurement techniques. Such attached spheres are termed colloid probes. Other advantages of AFM measurements are the possibility to use many types of materials for the colloid probes and plane surfaces, and the reduction of contamination problems due to the small area of contact between probe and plane surface.

The purpose of the present paper is to report systematic and reproducible data of the interaction forces between bovine serum albumin (BSA) layers adsorbed on a silica colloid probe and

* Corresponding author. Fax: +34 958 243214. E-mail: galisteo@ugr.es.

[†] University of Granada.

[‡] University of Málaga.

[§] Royal Institute of Technology.

on a silica flat surface. The forces between these layers were studied in a range of electrolyte concentrations, type of electrolyte, and solution pH values. Further, the force–distance curves measured have been quantitatively analyzed using the DLVO theory. Not only the electrostatic repulsive force and the van der Waals attractive force predicted by the DLVO theory appear in our system, but also the short-range repulsive force due to the adsorbed layer of water molecules and cations (hydration forces). The DLVO theory has been extended to include a hydration force term.

II. Materials and Methods

All chemicals used were of analytical grade quality. NaCl and CaCl₂ solutions were prepared with double-distilled water (Milli-Q System). The pH was controlled using different buffers (acetate at pH 5, phosphate at pH 7, borate at pH 9, at a constant ionic strength of 2 mM); a dilute HCl solution was used to keep the medium at pH 3.

The force measurements between BSA layers adsorbed on silica surfaces were performed using a Nanoscope III AFM (Digital Instruments, USA) and the colloid probe technique. The technique used in this study and the operation mode of the AFM are well-described in the literature.^{12,19–26} In brief, the colloid probe is held stationary and the flat surface is displaced in a controlled manner toward and away from the probe in an aqueous medium. The interaction forces between the probe and the flat surface can be obtained from the deflection of the cantilever which is monitored by a laser beam reflecting off the back of the cantilever to a split photodiode. The AFM software creates a file containing the output of the AFM versus the displacement of the flat surface. These raw data can be converted into a force versus separation curve by assuming a zero point for both the separation and the force. In order to scale the force measurements correctly, the spring constant of the cantilevers (which were standard V-shaped cantilevers without a tip) must be known accurately. A value of 0.09 N/m was achieved using the resonance method proposed by Cleveland et al.²⁷ Reported forces are normalized by the radius of the sphere attached to the cantilever.

Silica spheres, with a diameter of 5 μm, were supplied by Bangs Laboratory (USA). A colloidal silica particle was glued to the end of the cantilever using an optical microscope and a micromanipulator arm. Silica planes, with an area around 1 cm², were obtained from an oxidized silicon wafer (CSIC, Spain).

The BSA used in the experiments, supplied by Biokit (Spain), is a monomeric protein with an isoelectric point (iep) around 4.7.²⁸ This protein was adsorbed on silica surfaces (sphere and plane) to measure the interactions between BSA layers. With this aim 1 mg/mL of BSA solution (10 mM NaCl, pH 4.8) was injected in the AFM fluid cell, where the silica surfaces were immersed.^{29,30} The adsorption took place during 3 h at room temperature (22 °C). Finally, double-distilled water was injected to eliminate the nonadsorbed protein.

In all cases reported herein, the interaction force curves were very reproducible over many consecutive compression cycles at the same conditions of pH and NaCl concentration. This means that all the force curves obtained at the same medium conditions overlap each other. This fact evidences that the BSA was strongly adsorbed on the substrate surfaces. The pressure generated between the surfaces did not seem to induce any irreversible structural change in the adsorbed layers. The force curves obtained at certain conditions, even after changing the medium pH and salt concentration and going back to the original conditions (changes in pH from pH 9 to pH 3 and vice versa at

fixed salt concentration; changes in salt concentration from high value to low value and vice versa at fixed pH) were also very reproducible, which suggests that the protein did not desorb nor undergo irreversible conformational changes. In the same way, the reproducibility of the results was also very satisfactory after leaving the samples 9 h in a 10 mM NaCl and pH 5 medium.

III. Theoretical Background

The DLVO theory considers that the total potential energy V_T between two particles is given by

$$V_T = V_E + V_A \quad (1)$$

The attractive London–van der Waals energy V_A between a sphere and a plane is¹⁶

$$V_A = -\frac{AR}{6x} \quad (2)$$

where R is the particle radius, x is the distance between the surfaces of the sphere and the plane, and A is the Hamaker constant of the system. Equation 2 does not take the electro-magnetic delay into account.

The electrostatic energy V_E between a sphere and a plane under boundary conditions of constant surface potential (in the case of low surface potentials) is given by^{7,31,32}

$$V_E = \epsilon\pi R[(\Psi_s + \Psi_p)^2 \ln(1 + \exp(-\kappa x)) + (\Psi_s - \Psi_p)^2 \ln(1 - \exp(-\kappa x))] \quad (3)$$

where ϵ is the dielectric constant of the medium, Ψ_s is the surface potential of the sphere, Ψ_p is the surface potential of the plane, and κ is the inverse of the Debye length, which is given by the following equation:

$$\kappa = \sqrt{\frac{\sum_i n_i e^2 z_i^2}{\epsilon k T}} \quad (4)$$

with e being the electron charge, k the Boltzmann constant, T the absolute temperature, n_i the number concentration in the bulk of ions of type i , and z_i the valence of such ions.

In the case of boundary conditions of constant surface charge (and low surface potentials), the electrostatic energy V_E between a sphere and a plane is^{7,31,32}

$$V_E = -\epsilon\pi R[(\Psi_s + \Psi_p)^2 \ln(1 - \exp(-\kappa x)) + (\Psi_s - \Psi_p)^2 \ln(1 + \exp(-\kappa x))] \quad (5)$$

Since force versus separation curves are obtained in AFM experiments, it is useful to calculate the theoretical force by means of

$$F = -\frac{dV_T}{dx} \quad (6)$$

Thus, according to eqs 1, 2, 3, 5, and 6

$$\frac{F_{DLVO}}{R} = \frac{2\Psi_s\Psi_p \mp \exp(-\kappa x)(\Psi_s^2 + \Psi_p^2)}{1 - \exp(-2\kappa x)} - \frac{A}{6x^2} \quad (7)$$

TABLE 1: Best Fitting Parameters Obtained in the Fits of BSA–BSA Interaction Curves at Different pH Values, Salt Concentrations, and Salt Types^a

salt	concn	pH 3	pH 5	pH 7	pH 9
NaCl	0.01 M	$\Psi_S = \Psi_P = 20$ mV	$\Psi_S = \Psi_P = -7$ mV	$\Psi_S = \Psi_P = -15$ mV	$\Psi_S = \Psi_P = -16$ mV
	0.1 M	$\Psi_S = \Psi_P = 7$ mV	$\Psi_S = \Psi_P = -3$ mV	$\Psi_S = \Psi_P = -6$ mV	$\Psi_S = \Psi_P = -7$ mV
	1 M	$\Psi_S = \Psi_P = 0$ mV	$\Psi_S = \Psi_P = 0$ mV $C_H = 0.16$ mN/m $\lambda = 1.85$ nm	$\Psi_S = \Psi_P = 0$ mV $C_H = 0.20$ mN/m $\lambda = 1.85$ nm	$\Psi_S = \Psi_P = 0$ mV $C_H = 0.25$ mN/m $\lambda = 1.85$ nm
CaCl ₂	0.01 M	$\Psi_S = \Psi_P = 13$ mV	$\Psi_S = \Psi_P = -5$ mV	$\Psi_S = \Psi_P = -7$ mV	$\Psi_S = \Psi_P = -8$ mV
	0.05 M	$\Psi_S = \Psi_P = 7$ mV	$\Psi_S = \Psi_P = 0$ mV	$\Psi_S = \Psi_P = -3$ mV	$\Psi_S = \Psi_P = -4$ mV
	0.5 M	$\Psi_S = \Psi_P = 0$ mV		$\Psi_S = \Psi_P = 0$ mV $C_H = 0.10$ mN/m $\lambda = 2.25$ nm	$\Psi_S = \Psi_P = 0$ mV $C_H = 0.17$ mN/m $\lambda = 2.25$ nm

^a Equations 12 and 11 were used to fit the experimental data. In every case $s = 0$ nm.

The negative sign in the numerator of eq 7 corresponds to constant surface potential interaction and the positive sign to constant surface charge interaction. It is usual to normalize the measured surface force by the sphere radius in order to facilitate the comparison with the results obtained with other spheres of different sizes.

Equation 7 has been used to fit the experimental data, considering Ψ_S and Ψ_P as adjustable parameters. In all the cases studied in this article, the constant surface potential model fits the experimental data better than the constant surface charge model. Therefore, only the fits with the constant surface potential model will be shown in this paper. But in many cases it is necessary to introduce an additional term (a hydration term) to get a satisfactory fit of our results:

$$\frac{F}{R} = \frac{F_{DLVO}}{R} + \frac{F_{HYD}}{R} \quad (8)$$

The simplest expression for the hydration forces is the following empirical relation:¹⁶

$$\frac{F_{HYD}}{R} = C_H \exp\left(-\frac{x}{\lambda}\right) \quad (9)$$

where C_H is a hydration constant and λ is the decay length. Both parameters have been also considered as fitting parameters.

IV. Results and Discussion

BSA adsorption on the silica surfaces was performed to investigate the interactions between layers of this protein. The effects of pH and salt concentration in those interactions were analyzed. Figure 1 presents the interaction force profiles (approaching curves) between a BSA-coated colloid probe and a BSA-coated plane surface as a function of pH at low NaCl concentration (0.01 M NaCl). The interaction forces between silica surfaces covered with a BSA layer were weaker, that is less repulsive, than the forces between bare silica surfaces (results not shown). It is thus clear that adsorption of the BSA protein results in a decrease of charge.

When the medium pH is away from the isoelectric point (iep) of the protein (pHs 3, 7, and 9) the interaction between the adsorbed layers at large separations is dominated by an electrical double-layer repulsion. At short distances a strong repulsion attributed to steric forces owing to the overlap of adsorbed protein layers is observed. A higher double-layer repulsion at pH 3, when BSA is positively charged, than at pH 9 can be observed. At pH 5, near the iep of the protein, the electrostatic interaction is negligible. At a distance of around 4 nm, before the overlap of the protein layers, a small attraction is detected.

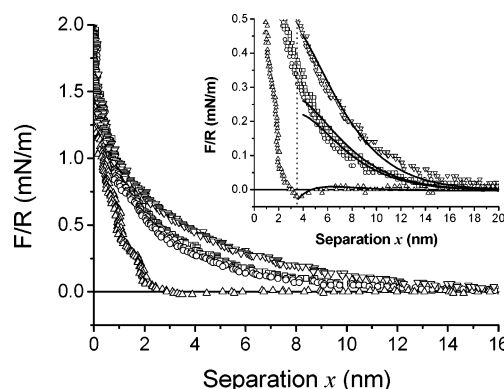


Figure 1. Normalized force vs separation distance x for BSA–BSA interaction in 0.01 M NaCl at different pHs: (\square) pH 9; (\circ) pH 7; (\triangle) pH 5; (∇) pH 3. The inset is a zoom of the graph. The lines are the DLVO theory predictions (eq 12). The fitting parameters are shown in Table 1.

At this pH a strong adhesion (intensity around 0.6 mN/m) also appears when the surfaces are separated (result not shown).

The lines in Figure 1 represent DLVO fits of the experimental data. Table 1 gives the value of the fitting parameters. In order to fit the experimental results, eqs 7 and 9 must be modified. The reason for such modification is the uncertainty in the origin of separation distances ($x = 0$ nm). One of the main disadvantages of the AFM is the impossibility of directly determining the separation distance between the interacting surfaces. This separation is inferred by considering that the surfaces are in contact (null separation, $x = 0$ nm) when they move jointly (“compliance region”). This is true when the surfaces are hard. But if there is a compressible layer on the surface, the situation of the plane $x = 0$ nm corresponds to the plane of maximum compression of the layer (see Figure 2); the thickness of that layer is experimentally inaccessible with the AFM. Therefore eqs 7 and 9 must be modified to include a displacement $2d$:

$$\frac{F_{DLVO}}{R} = 2\pi\epsilon\kappa \exp(-\kappa(x - 2d)) \times \frac{2\Psi_S\Psi_P \mp \exp(-\kappa(x - 2d))(\Psi_S^2 + \Psi_P^2)}{1 - \exp(-2\kappa(x - 2d))} - \frac{A}{6(x - 2d)^2} \quad (10)$$

$$\frac{F_{HYD}}{R} = C_H \exp\left(-\frac{(x - 2d)}{\lambda}\right) \quad (11)$$

There are two main difficulties associated with the evaluation of the van der Waals force between protein-coated surfaces. First, the Hamaker constant is not known with good precision

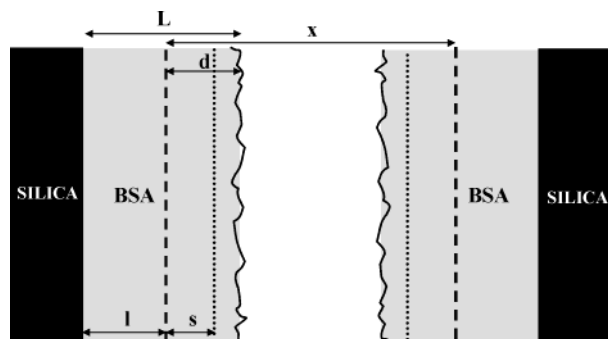


Figure 2. Schematic picture of the interaction between BSA layers. L is the thickness of the BSA layer; l is the thickness of the BSA layer at maximum compression; d is the distance between the layer surface and the plane of maximum compression (dashed plane); s is the distance between the origin plane of the London–van der Waals interaction (dotted plane) and the plane of maximum compression. L and l are inaccessible experimentally. The interaction between the BSA layers is measured as a function of the distance x (note that $x = 0$ nm at the plane of maximum compression).

because the dielectric properties of the protein layers depend on the water content and are thus hard to know exactly. Second, the protein layer/water interface is not smooth on a molecular scale. Thus, the origin plane of the London–van der Waals forces is not known with precision. In our analysis, therefore, the position of this plane respect to that of maximum protein layer compression ($x = 0$ nm) is determined by the parameter s (see Figure 2), which is obtained directly from the fit of the experimental results.

Just as is the case for the London–van der Waals forces, the origin plane for the electrical double-layer forces is not well-defined due to the molecular scale roughness of the surface of the protein layer. Ohshima et al.^{33,34} have proposed a potential distribution model for hard particles coated by an ion-penetrable charge surface layer, which has been used to describe the electrophoretic behavior of protein-coated particles.^{35–37} According to this model, when the surface-charged layer is thicker than the inverse of the Debye–Hückel parameter, the potential within the surface-charged layer is in practice equal to the surface potential at the boundary between the protein layer and the surrounding solution.^{38,39} As the electrical double-layer interaction is governed by the surface potential, we have assumed that the origin plane for the electrostatic repulsion corresponds to the limit of the protein layer.⁴⁰

With these assumptions, eq 10 is modified again to introduce a displacement between the origin planes for both interactions (electrostatic and van der Waals, see Figure 2):

$$\frac{F_{\text{DLVO}}}{R} = 2\pi\epsilon\kappa \exp(-\kappa(x - 2d)) \times \frac{2\Psi_s\Psi_p \mp \exp(-\kappa(x - 2d))(\Psi_s^2 + \Psi_p^2)}{1 - \exp(-2\kappa(x - 2d))} - \frac{A}{6(x - 2s)^2} \quad (12)$$

In all figures corresponding to protein–protein force profiles, separation distance equals zero ($x = 0$ nm) is defined as the point at which the protein layers are completely compressed. The parameter d was obtained from the interaction curve at pH 5 and 10 mM NaCl (Figure 1). In this curve a minimum (attraction) followed by the steric repulsion is observed. We have considered that the protein layers come into contact at the minimum position (that is, $2d = 3.5$ nm). According to this assumption, each protein layer is compressed 1.75 nm. This value was kept fixed in all the analyses. It is important to notice

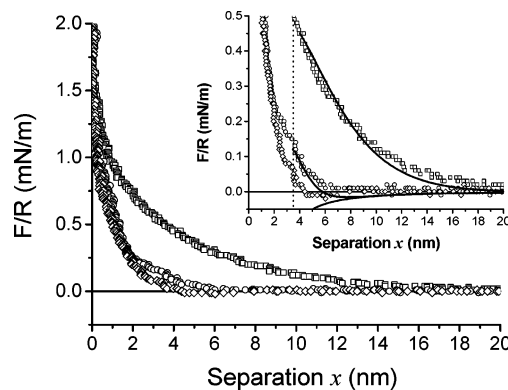


Figure 3. Normalized force vs separation distance x for BSA–BSA interaction at pH 3 as a function of NaCl concentration: (\square) 0.01 M; (\circ) 0.1 M; (\diamond) 1 M. The inset is a zoom of the graph. The lines are the DLVO theoretical fits according to eq 12. The fitting parameters are shown in Table 1.

that for globular proteins, such as BSA, the protein layer is only compressed by 1–2 nm before a hard wall is attained.⁴

The experimental data have been fitted until the point of contact of the BSA layers (distances $x \geq 3.5$ nm). A vertical dotted line at this point is introduced in all the figures to indicate this limit. Below that position the steric interaction comes into play. Currently the range and magnitude of this type of force cannot be modeled easily, and so theoretical predictions for this component are not included in the fits. The best fits were obtained considering electrostatic interaction under constant surface potential boundary conditions and with $s = 0$ nm. This value of s means that the origin plane of the van der Waals interaction coincides with the plane of maximum compression of the protein layer, in concordance with the assumption proposed by different authors in their SFA analysis.^{4,41} With this consideration we have found that a Hamaker constant for protein–water–protein of 7.5×10^{-21} J gave good fits to the experimentally determined forces. This value of the Hamaker constant is in agreement with the value used by Bowen et al.³⁰ It should be noticed that considering a constant value for the Hamaker constant we have implicitly assumed that the protein layer is a homogeneous phase with a uniform density. But this is strictly not true, especially in the outer parts of the protein layer. It could be acceptable to think that the contribution of the most external part of the protein layer to the London–van der Waals interaction should be somewhat smaller than the contribution of the rest of the protein layer due to a lower protein density in that region. However the net result could be the same as to consider an effective London–van der Waals interaction with a fixed value for the Hamaker constant and with the origin plane placed in the plane of maximum compression. This explanation is supported by the constant value of s ($s = 0$ nm). As can be seen in Figure 1, there is a close agreement between experiment and DLVO theory for all pH conditions.

Figure 3 shows the effect of NaCl concentration at pH 3. The force profiles presented in this figure are repulsive at large separation distances and decay exponentially as the separation distance increases. The decay length of the force was approximately equal to the theoretical Debye length for solutions of the ionic strength used in these experiments. Using the above approach, fits based on DLVO theory are shown in this figure. It can be seen that overall there is an acceptable agreement between the experiments and calculated forces. This agreement clearly demonstrates that the long-ranged forces observed in this system have an electrostatic origin, which corresponds to overlap of the electrical double layers emanating from the

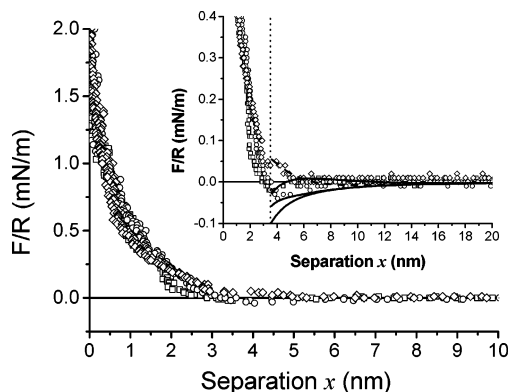


Figure 4. Normalized force vs separation distance x for BSA-BSA interaction at pH 5 as a function of NaCl concentration: (\square) 0.01 M; (\circ) 0.1 M; (\diamond) 1 M. The inset is a zoom of the graph. The solid lines represent the DLVO theory predictions, and the dashed line corresponds to the extended DLVO fit incorporating a hydration force term. The fitting parameters are shown in Table 1.

adsorbed BSA. An increase in salt concentration leads to a decrease in the range of electrostatic repulsion between the protein layers. At shorter separation distances for high salt concentration (1 M) the force becomes attractive under the influence of London-van der Waals interaction between the coated surfaces.

The interaction force data obtained between BSA-coated surfaces immersed in solutions at pH 5 containing different background NaCl concentrations are presented in Figure 4. At this pH, close to the iep of the protein (ca. 4.7), the electrostatic repulsion is negligible, and therefore no effect of salt concentration should be expected. However, the interaction force data obtained at 1 M are distinctly different from those obtained at lower salt concentrations (0.01 and 0.1 M). In these cases, the force profiles contain two force regimes, above and below a separation distance of approximately 4 nm. Above this distance there is practically no interaction. Because of the attractive van der Waals forces a minimum is observed at a surface separation of around 4 nm followed by a steric repulsion arising from compression of the adsorbed protein molecules. In the case of 1 M NaCl, the force profile does not present any minimum and the repulsion is more long-ranged. The data presented in this figure were analyzed in terms of the DLVO theory. As can be seen, the results for low electrolyte concentrations (0.01 and 0.1 M) are in good agreement with the DLVO predictions (solid lines). However, an important deviation occurs for high electrolyte concentration (1 M), where the experimental values of force are greater than the calculated. This observed extrarepulsion clearly appears at a separation prior to the protein layer overlap.

In general, the protein layer thickness depends on the electrolyte concentration.⁴² Proteins expand when the ionic strength is lowered because of an increased repulsion between protein charges. Therefore, the extrarepulsion observed at 1 M could not be attributed to steric repulsion because at this salt concentration proteins are less expanded than at lower ionic strength. If we bear in mind that the protein presents hydrophilic surfaces, it is plausible to suppose that this additional repulsion can be attributed to hydration forces. It is well established that water molecules strongly bind to protein surfaces.^{4,37,43} The hydration forces appear when proteins are negatively charged because under these conditions the counterions near the protein surface are the hydrated cations, which contribute with their hydration shell to the formation of a strongly bound water layer.⁴⁴ The larger quantity of cations at high salt concentrations

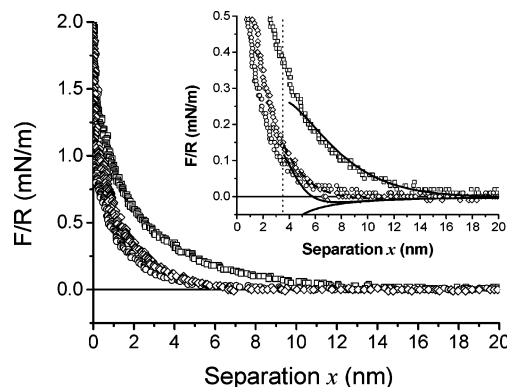


Figure 5. Normalized force vs separation distance x for BSA-BSA interaction at pH 9 as a function of NaCl concentration: (\square) 0.01 M; (\circ) 0.1 M; (\diamond) 1 M. The inset is a zoom of the graph. The solid lines represent the DLVO theory predictions, and the dashed line corresponds to the extended DLVO fit incorporating a hydration force term. The fitting parameters are shown in Table 1.

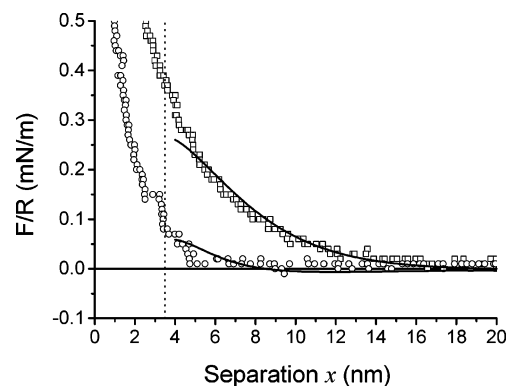


Figure 6. Normalized force vs separation distance x for BSA-BSA interaction at pH 9 obtained in 0.01 M NaCl (\square) and in 0.01 M CaCl_2 (\circ). The lines represent the DLVO theory predictions. The fitting parameters are shown in Table 1.

favors the appearance of hydration forces between proteins when the hydration layers overlap.^{45,46} This does not happen when the protein is positively charged ($\text{pH} < \text{iep}$) because the Cl^- anions (the counterions in this case) are practically not hydrated.¹⁶ We can see in Figure 4 that the measured force at 1 M NaCl agrees well with the extended DLVO prediction which include the hydration force term (dashed line).

The interaction forces between BSA-coated surfaces at pH 9 as a function of NaCl concentration are plotted in Figure 5 (similar results were obtained at pH 7). As shown, the measured forces are purely repulsive, no attractive forces are observed at any electrolyte concentration. It is noteworthy that the forces at 0.01 and 0.1 M NaCl can be fitted to the DLVO predictions (solid lines). The interaction profile at 1 M presents the non-DLVO force before the protein layers overlap, which may be fitted with the extended DLVO theory (dashed line).

In the last part of this paper we present a study of the interaction between BSA-coated silica surfaces in the presence of CaCl_2 as electrolyte. Figure 6 compares the force curves obtained at pH 9 in a 0.01 M NaCl solution and in a 0.01 M CaCl_2 solution. Both can be fitted to the DLVO theory. It should be noted here that the effect of salt type corroborates the electrostatic nature of the protein interaction at low salt concentration. The presence of CaCl_2 in the medium instead of NaCl causes a larger screening of the electrostatic interaction and even an adhesion when surfaces are separated (data not shown). Figure 7 shows the results of the force measurements performed at pH 5 in a 0.01 M NaCl solution and in a 0.01 M

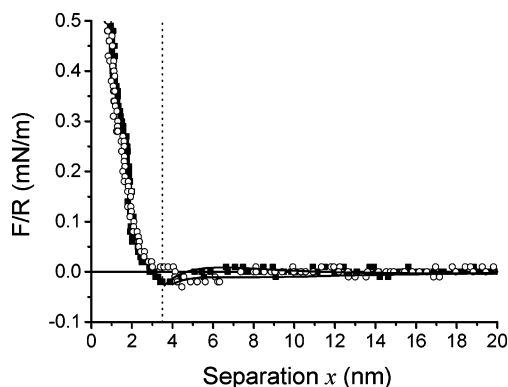


Figure 7. Normalized force vs separation distance x for BSA-BSA interaction at pH 5 obtained in 0.01 M NaCl (■) and in 0.01 M CaCl_2 (○). The lines represent the DLVO theory predictions. The fitting parameters are shown in Table 1.

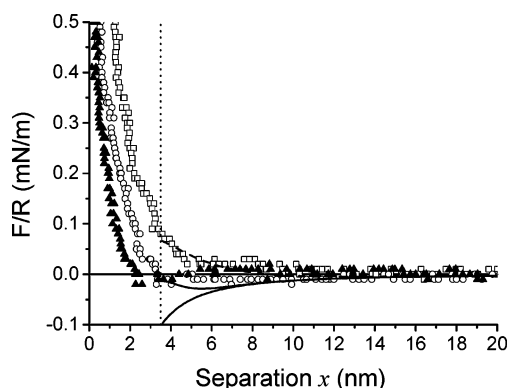


Figure 8. Effect of the CaCl_2 concentration on the BSA-BSA interaction at different experimental conditions: (○) 0.05 M pH 9; (□) 0.5 M pH 9; (▲) 0.5 M pH 3. The solid lines represent the DLVO theory predictions, and the dashed line corresponds to the extended DLVO fit incorporating a hydration force term. The fitting parameters are shown in Table 1.

CaCl_2 solution. It is clear that the interaction curves are identical, and both can be satisfactorily fitted by the DLVO theory. At this pH the negligible electrostatic interaction leads to an absence of any effect of salt type. Finally, Figure 8 presents the forces measured with changing CaCl_2 concentration at pH 9 and pH 3. Clearly, the decay length increases with increasing CaCl_2 concentration at pH 9, contrary to the behavior expected with pure electrostatic interaction. Attempts were made to fit the data to the DLVO theory. The force curve for low electrolyte concentration conforms quite well to conventional DLVO theory. However, for 0.5 M and pH 9 only the data obtained at large separations can be fitted to the theory. A weak repulsive force appears at a separation below 8 nm, which could be attributed to the existence of hydration forces. This type of interaction is not observed in the case of the same electrolyte concentration at pH 3, showing a clear difference between pH values above or below the iep of BSA. The force data obtained at short separations for 0.5 M and pH 9 have been fitted to the extended DLVO theory, shown by the dashed line in Figure 8, with the hydration force parameters given in Table 1. We can observe a good correlation between this fit and the experimental values.

The parameter values which lead the best theoretical fits in each condition are listed in Table 1. Analysis of these data provides useful information, such as the relative low surface potential of BSA layers. In addition, it can be observed how the surface potential of the BSA layer at low salt concentration increases (in absolute value) away from the iep of BSA. Of

course this surface potential is reduced as the concentration of the background electrolyte is increased from 0.01 to 1 M, in line with expectations based on the surface charging behavior of other less complex surfaces.³¹ Also it can be noticed that the surface potential diminishes in the case when more screening salt (CaCl_2) is present in the medium.

At high salt concentration and at pH above the iep of BSA, hydration forces appear. Table 1 also includes the hydration force parameters C_H and λ . The explanation of the existence of this extraneous repulsion observed in BSA-coated surfaces may be that the water structure in the vicinity of the BSA layer changes significantly in the presence of high electrolyte concentration. It is possible that cations specifically adsorb on the protein layer and cause changes in the structure of the adjacent water. Note that the value for λ only depends on the salt type. It is consistent that this parameter, related to the size of the hydrated cations and the thickness of the water layer around the hydrophilic surfaces, is higher in the case of CaCl_2 (Ca^{2+} is a more hydrated and bigger cation than Na^+). In addition, the intensity of the hydration forces increases (C_H grows) as the pH increases: the more negatively charged the BSA surface (the higher the pH) the more hydrophilic is the surface (and the greater is the adsorption of cations). It is noteworthy that the values of λ match within the ranges found in the literature (between 0.1 and 2.2 nm).^{16,47} The values found in the literature for C_H , corresponding to very hydrophilic surfaces, range from 1.2 mN/m for quartz to 40 mN/m for mica.^{16,47} In our case the value of C_H is quite low because a protein layer is not as hydrophilic as silica or mica.

Now it may be opportune to make some comments about the fitting parameters. First of all, it can be observed in Table 1 that Ψ_S and Ψ_P coincide in every case. Although we have treated these magnitudes as independent parameters, the fitting procedure leads to the same value for them. This fact, probably due to the symmetry of eq 12, makes sense since both surfaces (the sphere and the plane) are of the same nature. Therefore, these two parameters can be considered effectively as one. On the other hand, it is necessary to emphasize that eqs 7 and 12 are valid only at low surface potential $\psi_o < (kT/ze)$, a condition that is fulfilled in all cases.

Another observation is the fact of the satisfactory fits obtained with a low number of adjustable parameters. At low salt concentration only one adjustable parameter was used: the surface potential. At high salt concentration two adjustable parameters were employed: C_H and λ , which characterized the hydration interaction. Although strictly speaking another parameter was used (the distance s), the constant value of this in all cases seems to suggest that this is a fixed, rather than a variable, fitting parameter.

Bowen et al. have also studied the interaction between BSA layers adsorbed on silica surfaces with an AFM.³⁰ Their measurements were carried out at pH 8 and 6 and at NaCl concentrations below 0.1 M. This is why they did not observe van der Waals attraction nor hydration forces: the salt concentration was not high enough and measurements at pH below the iep of BSA were not performed. The surface potentials obtained in their work are higher than our results probably because they used a different theoretical treatment.

V. Conclusions

The interaction forces between BSA layers (adsorbed on silica surfaces) in aqueous media at different pH and salt concentrations were directly measured with an AFM.

Electrostatic and steric forces are the dominant interactions between BSA layers at low salt concentrations. Electrical

double-layer repulsion dominates the interaction at large separation distances when the BSA molecules are charged, while at short separations a steric repulsion due to the compression of the adsorbed protein layers appears. The measured force-distance curves obtained in a variety of pH values at low electrolyte concentration were in good quantitative agreement with predictions based on the DLVO theory.

The results presented in this paper suggest that a short-range repulsive force, different from the steric interaction between protein layers, appears at pH values above the isoelectric point of BSA and at high electrolyte concentrations. This force may be attributed to the existence of hydration forces, related to counterion-assisted structuring of the water in the vicinity of the protein molecules. The short-range repulsive hydration forces could be observed in the presence of high concentrations of Na^+ or Ca^{2+} and varied in magnitude with pH and cation type. The measured forces have been satisfactorily fitted to the extended DLVO theory, where a hydration term has been included. The conclusions of this work are in agreement with experimental results previously obtained about the colloidal stability of protein-coated particles.^{37,45,46}

It has been shown that intermolecular repulsion may be present in protein solutions even at high electrolyte concentrations at which electrostatic interactions are suppressed. This could explain the stability of proteins at high salt concentration and the necessity for additives such as Cd^{2+} to induce crystallization.⁴⁸

This paper shows how the AFM colloid probe technique can provide a useful means of directly quantifying the interaction between biological macromolecules.

Acknowledgment. This work was supported by the Spanish "Technology and Science Ministry" (Projects MAT 99-0662-C03-02, MAT 2001-1743, and AGL 2001-3843-C02-02) and by a Grant of the same Ministry to J.J.V.D.

References and Notes

- (1) Zubay, G. *Biochemistry*; Addison-Wesley: Reading, MA, 1983.
- (2) Feurstein, I. A.; Ratner, B. D. *Biomaterials* **1990**, *11*, 127.
- (3) Murro, M. S.; Ebherbart, R. C.; Maki, N. J.; Brink, B. E.; Frye, R. L. *Am. Soc. Artif. Intern. Organs J.* **1983**, *6*, 65.
- (4) Claesson, P. M.; Blomberg, E.; Fröberg, J. C.; Nylander, T.; Arnebrant, T. *Adv. Colloid Interface Sci.* **1995**, *57*, 161.
- (5) Israelachvili, J. N.; Adams, G. E. *J. Chem. Soc., Faraday Trans. 1* **1978**, *74*, 975.
- (6) Derjaguin, B. V.; Landau, L. *Acta Physicochim. USSR* **1941**, *14*, 633.
- (7) Verwey, E. J. W.; Overbeek, J. T. G. *Theory of the Stability of Lyophobic Colloids*; Elsevier: Amsterdam, 1952; Vols. 1 and 2.
- (8) Israelachvili, J. N.; Pashley, R. M. *Nature* **1982**, *300*, 341.
- (9) Rabinovich, Y. I.; Derjaguin, B. V. *Colloids Surf.* **1988**, *30*, 243.
- (10) Pashley, R. M.; McGuiggan, P. M.; Ninham, B. W.; Evans, D. F. *Science* **1985**, *229*, 1088.
- (11) Grabbe, A.; Horn, R. G. *J. Colloid Interface Sci.* **1993**, *157*, 375.
- (12) Ducker, W. A.; Senden, T. J.; Pashley, R. M. *Nature* **1991**, *353*, 239.
- (13) Horn, R. G.; Smith, D. T.; Haller, W. *Chem. Phys. Lett.* **1989**, *162*, 404.
- (14) Rabinovich, Y. I.; Derjaguin, B. V.; Churaev, N. V. *Adv. Colloid Interface Sci.* **1982**, *16*, 63.
- (15) Peschel, G.; Belouschek, P.; Muller, M. M.; Muller, M. R.; Konig, R. *Colloid Polym. Sci.* **1982**, *260*, 444.
- (16) Israelachvili, J. N. *Intermolecular and Surface Forces*, 2nd ed.; Academic Press: London, 1991.
- (17) Derjaguin, B. V.; Churaev, N. V. *Colloids Surf.* **1989**, *41*, 223.
- (18) Butt, H. J. *Biophys. J.* **1991**, *60*, 1438.
- (19) Binnig, G.; Quate, C. F.; Gerber, Ch. *Phys. Rev. Lett.* **1986**, *56*, 930.
- (20) Ducker, W. A.; Senden, T. J.; Pashley, R. M. *Langmuir* **1992**, *8*, 1831.
- (21) Giesbers, M. *Surface Forces Studied with Colloidal Probe Atomic Force Microscopy*. Ph.D. Thesis, University of Wageningen, The Netherlands, 2001.
- (22) Zhmud, B. V.; Meurk, A.; Bergström, L. *J. Colloid Interface Sci.* **1998**, *207*, 332.
- (23) Toikka, G.; Hayes, R. A. *J. Colloid Interface Sci.* **1997**, *191*, 102.
- (24) Hartley, P. G.; Larson, I.; Scales, P. J. *Langmuir* **1997**, *13*, 2207.
- (25) Rutland, M. W.; Senden, T. J. *Langmuir* **1993**, *9*, 412.
- (26) Claesson, P. M.; Ederth, T.; Bergeron, V.; Rutland, M. W. *Adv. Colloid Interface Sci.* **1996**, *67*, 119.
- (27) Cleveland, J. P.; Manne, S.; Bocek, D.; Hansma, P. K. *Rev. Sci. Instrum.* **1993**, *64*, 403.
- (28) Peula-García, J. M.; Hidalgo-Álvarez, R.; de las Nieves, F. J. *Colloid Polym. Sci.* **1997**, *275*, 198.
- (29) Fukuzaki, S.; Urano, H.; Nagata, K. *J. Ferment. Bioeng.* **1996**, *81*, 163.
- (30) Bowen, W. R.; Hilal, N.; Lovitt, R. W.; Wright, C. J. *J. Colloid Interface Sci.* **1998**, *197*, 348.
- (31) Hunter, R. J. *Foundations of Colloid Science*; Oxford University Press: New York, 1987, Vol. 1.
- (32) Puertas-López, A. M. *Aggregation in Mesoscopic Systems Controlled by Long-Range Attractive Interactions*. Ph.D. Thesis, University of Granada, Spain, 1999.
- (33) Ohshima, H.; Ohki, S. *Biophys. J.* **1985**, *47*, 673.
- (34) Ohshima, H.; Nakamura, M.; Kondo, T. *Colloid Polym. Sci.* **1992**, *270*, 873.
- (35) Nakamura, M.; Ohshima, H.; Kondo, T. *J. Colloid Interface Sci.* **1992**, *154*, 393.
- (36) Ortega-Vinuesa, J. L.; Martín-Rodríguez, A.; Hidalgo-Álvarez, R. *Colloids Surf., A: Physicochem. Eng. Aspects* **1995**, *95*, 261.
- (37) Molina-Bolívar, J. A.; Galisteo-González, F.; Hidalgo-Álvarez, R. *Colloids Surf., B: Biointerfaces* **2001**, *21*, 125.
- (38) Sakuma, S.; Ohshima, H.; Kondo, T. *J. Colloid Interface Sci.* **1989**, *133*, 253.
- (39) Sakuma, S.; Ohshima, H.; Kondo, T. *J. Colloid Interface Sci.* **1990**, *135*, 455.
- (40) Ohnishi, S.; Murata, M.; Hato, M. *Biophys. J.* **1998**, *74*, 455.
- (41) Blomberg, E.; Claesson, P. M.; Fröberg, J. C. *Biomaterials* **1998**, *19*, 371.
- (42) Belfort, G.; Lee, C. S. *Proc. Natl. Acad. Sci. U.S.A.* **1991**, *88*, 9146.
- (43) Bellissent-Funel, M. C. *J. Mol. Liq.* **2000**, *84*, 39.
- (44) Pashley, R. M. *Adv. Colloid Interface Sci.* **1982**, *16*, 57.
- (45) Molina-Bolívar, J. A.; Galisteo-González, F.; Hidalgo-Álvarez, R. *Phys. Rev. E* **1997**, *55*, 4522.
- (46) Molina-Bolívar, J. A.; Ortega-Vinuesa, J. L. *Langmuir* **1999**, *15*, 2644.
- (47) Škvarla, J.; Kmet', S. *Intern. J. Miner. Process.* **1991**, *32*, 111.
- (48) Thomas, B. R.; Carter, D.; Rosenberger, F. J. *Cryst. Growth* **1998**, *187*, 499.